Comput Visual Sci
DOI 10.1007/s00791-008-0112-2

REGULAR ARTICLE

Comparison study for Level set and Direct Lagrangian methods for computing Willmore flow of closed planar curves

Michal Beneš · Karol Mikula · Tomáš Oberhuber · Daniel Ševčovič

Received: 31 January 2007 / Accepted: 29 August 2007

Abstract The main goal of this paper is to present results of comparison study for the level set and direct Lagrangian methods for computing evolution of the Willmore flow of embedded planar curves. To perform such a study we construct new numerical approximation schemes for both Lagrangian as well as level set methods based on semi-implicit in time and finite/complementary volume in space discretizations. The Lagrangian scheme is stabilized in tangential direction by the asymptotically uniform grid point redistribution. Both methods are experimentally second order accurate. Moreover, we show precise coincidence of both approaches in case of various elastic curve evolutions provided that solving the linear systems in semi-implicit level set method is done in a precise way, redistancing is performed occasionally and the influence of boundary conditions on the level set function is eliminated.

Keywords Elastic curve · Willmore flow · Level set method · Lagrangian method · Tangential redistribution · Semi-implicit scheme · Complementary volume method

Mathematics Subject Classification (2000) 35K55 · 53C44 · 65M60 · 74S05

Communicated by P. Frolkovic.

The authors were partly supported by the following projects and grants: the project HPC-EUROPA(RII3-CT-2003-506079), the NCMM project LC06052, VEGA 1/3321/06 grant, the project MSM 6840770010 and APVV-0247-06, APVV-RPEU-0004-06 grants.

M. Beneš · T. Oberhuber (✉)
Department of Mathematics, Faculty of Nuclear Sciences and Physical Engineering, Czech Technical University in Prague, Trojanova 13, 120 00 Praha 2, Czech Republic
e-mail: oberhuber@kmlinux.fjfi.cvut.cz

M. Beneš
e-mail: benesm@kmlinux.fjfi.cvut.cz

K. Mikula
Department of Mathematics, Slovak University of Technology, Radlinského 11, 813 68 Bratislava, Slovak Republic
e-mail: mikula@vox.svf.stuba.sk

D. Ševčovič
Department of Applied Mathematics and Statistics, Faculty of Mathematics, Physics and Informatics, Comenius University, 842 48 Bratislava, Slovak Republic
e-mail: sevcovic@fmph.uniba.sk

1 Introduction

In the past years, elastic curves, the Willmore functional and the corresponding gradient flow (the Willmore flow) attracted a lot of attention from both theoretical as well as computational point of view. Following Daniel Bernoulli's model of an elastic rod, a classical elastica is a curve Γ in the plane which is a critical point (minimizer) for the elastic energy functional

$$E(\Gamma) = \frac{1}{2}\int_{\Gamma} k^2 \,\mathrm{d}s. \tag{1}$$

The first comprehensive study of analytical properties of non-closed planar curves that are minimizers to (1) goes back to Leonhard Euler who presented their characterization and classification in the pioneering work Additamentum I (De Curvis Elasticae) contained in his Opera Omnia [11]. Since then much effort has been spent to analyze and provide complete characterization of both minimizers to (1) as well as solutions corresponding to the gradient flow associated with the elastic energy functional (1). It is well known from Euler's

work that the flow of planar curves with the normal velocity given by

$$\beta = -\partial_s^2 k - \frac{1}{2}k^3 \tag{2}$$

is a gradient flow for the elastic energy functional $E(\Gamma)$ (see e.g. [7,10]). Such fourth order flows of closed curves and its 3D analogies appear in various physical and computer vision applications dealing with a motion of phase interfaces or with an image and surface reconstructions [4–6,10,15,22,25].

We remind ourselves that the so-called surface diffusion problems (see e.g. [2,20]) are described by nonstationary 4^{th} order intrinsic partial differential equations. Similarly, a numerical solution to the Willmore flow, either in direct (Lagrangian) or level set (Eulerian) formulation, is a nontrivial problem and leads to a solution of fourth order in space nonlinear evolution PDEs Convergence of a semidiscrete time continuous finite element discretization in the case when the evolved surface is a graph has been proved by Dziuk and Deckelnick in [8]. First numerical study based on the finite element method for the Willmore flow in Lagrangian formulation was presented in [10] and for the level set formulation in [9]. Finite difference discretization has been analyzed in [1,21]. Tangential stabilization of Lagrangian approach for solving fourth order elastic curve flows in case of surface diffusion was first introduced in [20]. Then a parametric finite element method was tangentially stabilized in [3]. Although the Lagrangian methods are fast and robust (when incorporating a suitable tangential velocity) they cannot handle topological changes for which the level set methods are preferred [9,22]. However, a careful and systematic comparison of nontrivial examples of direct and level set approaches for fourth order curve evolution problems is still missing. The goal of this paper is to provide such a comparison study, and, moreover to derive new numerical schemes based on the finite/complementary volume strategies for both Lagrangian and level set formulations of the Willmore flow.

First, we present a tangentially stabilized Lagrangian method based on a solution to the curvature, local length and position vector equations accompanied by the asymptotically uniform tangential redistribution of numerical grid points. We show experimentally that the method is second order accurate. We apply this method to various examples of evolution of planar embedded curves. Stabilization by the tangential velocity allows us to use reasonable large computational time steps and prevent formation of various instabilities like merging of evolving curve representing grid points or swallow tails, which are typical disadvantages of the direct methods.

Then we develop new semi-implicit complementary volume scheme for solving level set formulation of the Willmore flow. It is again second order accurate. Due to a finite volume character of discretization it has a potential to be naturally connected with finite volume schemes for advective level set equations [12,13] and thus to be used in various models where the fourth order terms serve as a curve motion regularization arising, e.g., in image segmentations [25].

The outline of the paper is as follows. In Sect. 2.1 we recall a closed governing system of equations for the curvature, local length and position vector describing evolution of plane curves satisfying (2) in Lagrangian formulation and describe the main idea of asymptotically uniform tangential redistribution. Section 2.2 focuses on the brief derivation of the governing equation representing the evolution of zero level set satisfying the geometric equation (2). In Sect. 3.1 we present our Lagrangian numerical approximation scheme and, in Sect. 3.2, approximation of the level set equation for the Willmore flow. Section 4 is devoted to study of the experimental order of convergence for both methods and to comparison of both methods in various elastic curve evolution examples.

2 Governing equations

2.1 Direct Lagrangian method

Henceforth we shall parameterize an embedded regular plane curve Γ by a smooth function $x : S^1 \to \mathbb{R}^2$, i.e. $\Gamma = \text{Image}(x) := \{x(u), u \in S^1\}$ such that the local length element $g = |\partial_u x| > 0$ is everywhere positive. Taking into account the periodic boundary conditions at $u = 0, 1$ we shall hereafter identify S^1 with the interval $[0, 1]$. The unit arc-length parameterization will be denoted by s, so $\mathrm{d}s = g\,\mathrm{d}u$. The tangent vector $\mathbf{T}$ and the signed curvature k of Γ satisfy $\mathbf{T} = \partial_s x = \partial_u x/g$, $k = \partial_s x \wedge \partial_s^2 x = \partial_u x \wedge \partial_u^2 x/g^3$. Moreover, we choose the unit inward normal vector $\mathbf{N}$ such that $\mathbf{T} \wedge \mathbf{N} = 1$ where $\mathbf{a} \wedge \mathbf{b}$ is the determinant of the 2×2 matrix with column vectors $\mathbf{a}$, $\mathbf{b}$. By ν we denote the tangent angle to Γ, i.e. $\mathbf{T} = (\cos\nu, \sin\nu)^T$. Now it follows from Frenét's formulae that $\partial_s \mathbf{T} = k\mathbf{N}$, $\partial_s \mathbf{N} = -k\mathbf{T}$ and $\partial_s \nu = k$. Notice that the curvature k is positive for convex closed curves in our convention of picking of normal and tangent vector orientation.

Let a regular smooth initial curve $\Gamma_0 = \text{Image}(x_0)$ be given. According to [17], an evolving family of planar curves $\Gamma_t = \text{Image}(x(.,t))$, $t \in [0, T)$, satisfying (2) can be represented by a solution to the following system of PDEs

$$\partial_t k = \partial_s^2 \beta + \alpha \partial_s k + k^2 \beta, \tag{3}$$

$$\partial_t g = -gk\beta + g\partial_s \alpha, \tag{4}$$

$$\partial_t x = \beta \mathbf{N} + \alpha \mathbf{T}, \tag{5}$$

subject to initial conditions $k(.,0) = k_0$, $g(.,0) = g_0$, and $x(.,0) = x_0(.)$,. We impose periodic boundary conditions at $u = 0, 1$. Having recalled the general form of governing

equations we are able to calculate the time derivative of the elastic energy functional

$$2\frac{\mathrm{d}}{\mathrm{d}t}E(\Gamma_t) = \frac{\mathrm{d}}{\mathrm{d}t}\int_0^1 k^2 g\,\mathrm{d}u = \int_{\Gamma_t} 2k\partial_t k - k^3\beta + k^2\partial_s\alpha\,\mathrm{d}s.$$

Since $\int_{\Gamma_t} k\partial_s^2\beta = \int_{\Gamma_t}\beta\partial_s^2 k$ and $\int_{\Gamma_t}\partial_s(\alpha k^2) = 0$ we obtain the following equation

$$\frac{\mathrm{d}}{\mathrm{d}t}E(\Gamma_t) = \int_{\Gamma_t}(\partial_s^2 k + \frac{1}{2}k^3)\beta\,\mathrm{d}s. \tag{6}$$

It enables us to conclude that the evolution of Γ_t with the normal velocity $\beta = -\partial_s^2 k - \frac{1}{2}k^3$ is a gradient flow (the Willmore flow) for the Willmore elastic energy functional E.

Notice that the tangential velocity α is a free parameter in (3)–(5) and it may depend on other quantities like e.g. the curvature, normal velocity and/or local length element in various ways including local or nonlocal dependences, cf. [14,16–19]. In this paper we make use of the so-called asymptotically uniform tangential redistribution derived in [18,19] which is the most natural for the Willmore flow since an initial shape is approaching evolution of expanding circles. Let us denote $L = L_t$ the total length of a curve Γ_t. It follows from analysis of the tangential velocity made in [18,19] that

$$\frac{g(u,t)}{L_t} \to 1 \quad \text{as } t \to T_{max} \quad \text{uniformly w.r. to } u \in S^1$$

provided that the tangential velocity is a solution to a nonlocal equation

$$\partial_s\alpha = k\beta - \langle k\beta\rangle_\Gamma + (L/g - 1)\,\omega,\ \alpha(0,t) = 0. \tag{7}$$

Here $\omega > 0$ is a given positive constant and $\langle . \rangle_\Gamma$ is an averaging operator over a curve Γ, i.e. $\langle k\beta\rangle_\Gamma = \frac{1}{L}\int_\Gamma k\beta\,\mathrm{d}s$. It is clear that redistribution of grid points along a curve becomes uniform as t approaches the maximal time of existence T_{max}. In the case of a Willmore flow the time horizon is infinite (i.e. $T_{max} = +\infty$) for planar Jordan curves and T_{max} can be finite for some selfintersecting immersed curves in the plane. Furthermore, inserting α computed from (7) into (3)–(5) and making use of the identity $\alpha\partial_s k = \partial_s(\alpha k) - k\partial_s\alpha$ then the curvature and local length equations can be rewritten as follows

$$\partial_t k = \partial_s^2\beta + \partial_s(\alpha k) + k\langle k\beta\rangle_\Gamma + (1 - L/g)\,k\omega, \tag{8}$$

$$\partial_t g = -g\langle k\beta\rangle_\Gamma + (L - g)\omega. \tag{9}$$

In other words, the strong "point-wise" influence of the term $k\beta$ in (3) and (4) has been softened by the "averaged" term $\langle k\beta\rangle_\Gamma$ in (8) and (9). As a consequence, this important property of asymptotically uniform tangential velocity enables us to construct an efficient and stable numerical scheme preventing fast local decrease of local lengths (merging of numerical grid points) as well as forming various further numerical instabilities related to high local curvature. Since

$$\begin{aligned}\partial_s^4 x &= \partial_s^3\mathbf{T} = \partial_s^2(k\mathbf{N})\partial_s^2 k\mathbf{N} + 2\partial_s k\partial_s\mathbf{N} + k\partial_s^2\mathbf{N}\\ &= \partial_s^2 k\mathbf{N} - 2(\partial_s k)k\mathbf{T} - k\partial_s(k\mathbf{T})\\ &= \partial_s^2 k\mathbf{N} - 3k(\partial_s k)\mathbf{T} - k^2\partial_s\mathbf{T}\\ &= \partial_s^2 k\mathbf{N} - \frac{3}{2}\partial_s(k^2)\partial_s x - k^2\partial_s^2 x\end{aligned}$$

and $\partial_s^2 x = k\mathbf{N}$ we have

$$\begin{aligned}(-\partial_s^2 k - \frac{1}{2}k^3)\mathbf{N} &= -\partial_s^4 x - \frac{3}{2}k^2\partial_s^2 x - \frac{3}{2}\partial_s(k^2)\partial_s x\\ &= -\partial_s^4 x - \frac{3}{2}\partial_s(k^2\partial_s x).\end{aligned}$$

Thus the governing system of Eqs. (3)–(5) for the Willmore flow (2) with tangential redistribution can be written as follows:

$$\partial_t k = -\partial_s^4 k - \frac{1}{2}\partial_s^2(k^3) + \partial_s(\alpha k) + k(k\beta - \partial_s\alpha), \tag{10}$$

$$\partial_t\eta = -k\beta + \partial_s\alpha, \quad \eta = \ln(g), \tag{11}$$

$$\partial_t x = -\partial_s^4 x - \frac{3}{2}\partial_s(k^2\partial_s x) + \alpha\partial_s x \tag{12}$$

where the tangential velocity α is the unique solution to Eq. (7).

2.2 Level set method

In the level set method the evolving family of planar curves $\Gamma_t, t \geq 0$, is represented by the zero level set of the so-called shape function $u : \Omega \times [0,T] \to \mathbb{R}$ where $\Omega \subset \mathbb{R}^2$ is a simply connected domain containing the whole family of evolving curves $\Gamma_t, t \in [0,T]$. Assuming zero is the regular value of the mapping $u(.,t)$, i.e. $|\nabla u(x,t)| \neq 0$ for $u(x,t) = 0$ we can express the unit inward normal vector and signed curvature as: $\mathbf{N} = \nabla u/|\nabla u|$ and $k = -\mathrm{div}\,(\nabla u/|\nabla u|)$. Let us denote the following auxiliary functions:

$$H = \mathrm{div}\left(\frac{\nabla u}{|\nabla u|}\right),\ Q = |\nabla u|,\ w = QH.$$

Then $\partial_s k = -\nabla H.\partial_s x = -\nabla H.\mathbf{T}$ and, by Frenét's formula, $\partial_s^2 k = -k\nabla H.\mathbf{N} - \mathbf{T}^t\nabla^2 H\mathbf{T}$. Differentiating the equation $u(x(s,t),t) = 0$ with respect to time we obtain $\partial_t u + \nabla u.\partial_t x = 0$. Since the normal velocity of x is $\beta = \partial_t x.\mathbf{N}$ we obtain $\frac{1}{|\nabla u|}\partial_t u = -\beta$. Inserting expressions for $\partial_s^2 k$ and $k = -H$ we obtain

$$\frac{1}{Q}\partial_t u = \frac{1}{2}\mathrm{div}\left(\frac{H^2}{Q}\nabla u\right) - H^3 - \mathbf{T}^t\nabla^2 H\mathbf{T}.$$

Here $\mathbf{T} = (-n_2, n_1)$ where $\mathbf{N} = (n_1, n_2)$, i.e. $\mathbf{T}$ is the vector $\mathbf{N}$ rotated by $-\pi/2$. Straightforward calculations show that the right hand side of the above equation can be rewritten

in the divergent form. The resulting system of two equations governing the evolution of the shape function has been derived by Droske and Rumpf in [9] and it reads as follows:

$$\partial_t u = -Q \operatorname{div}\left(\mathbb{E}\nabla w - \frac{1}{2}\frac{w^2}{Q^3}\nabla u\right), \tag{13}$$

$$w = Q \operatorname{div}\left(\frac{\nabla u}{|\nabla u|}\right) \tag{14}$$

where the 2×2 matrix $\mathbb{E} = \frac{1}{Q}\left(\mathbb{I} - \frac{\nabla u}{Q}\otimes\frac{\nabla u}{Q}\right)$ is a projection into a tangential space of the curve representing the zero level set of u. System of Eqs. (13–14) is subject to the initial condition

$$u(x,0) = u^0(x), \quad x \in \Omega$$

and clamped boundary conditions at $\partial\Omega$, i.e. $u(x,t) = 0$, $\partial_v u(x,t) = 0$, $x \in \partial\Omega$. The initial function u^0 is a signed distance function, i.e. $u^0(x) = \operatorname{dist}(x, \Gamma^0)$, $x \in \Omega$.

3 Numerical approximation schemes

3.1 Numerical approximation of the Lagrangian method

Our numerical approximation of an evolved curve is represented by discrete plane points x_i^j where the index $i = 1,\ldots,n$, denotes space discretization and the index $j = 0,\ldots,m$, stands for a discrete time stepping. Due to periodic boundary conditions we use additional values $x_{-1}^j = x_{n-1}^j$, $x_0^j = x_n^j$, $x_{n+1}^j = x_1^j$, $x_{n+2}^j = x_2^j$. If we take a uniform division of the time interval $[0,T]$ with a time step $\tau = \frac{T}{m}$ and a uniform division of the fixed parameterization interval $[0,1]$ with a step $h = 1/n$, a point x_i^j corresponds to $x(ih, j\tau)$. The systems of difference equations corresponding to (7), (10)–(12) will be solved for discrete quantities α_i^j, η_i^j, r_i^j, k_i^j, x_i^j, $i = 1,\ldots,n$, $j = 1,\ldots,m$, representing approximations of the unknowns α, η, gh, k and x, respectively. Here α_i^j represents the tangential velocity of a flowing node x_i^j, and $\eta_i^j, r_i^j \approx |x_i^j - x_{i-1}^j|$ and k_i^j represent piecewise constant approximations of the corresponding quantities in the so-called flowing finite volume $\left[x_{i-1}^j, x_i^j\right]$. In order to derive new position x_i^j we use corresponding flowing dual volumes $\left[\tilde{x}_{i-1}^j, \tilde{x}_i^j\right]$ where $\tilde{x}_i^j = \frac{x_{i-1}^j + x_i^j}{2}$ with approximate lengths $q_i^j \approx |\tilde{x}_{i+1}^j - \tilde{x}_i^j|$. Our computational method is simple and natural. At the j-th discrete time step, we first find values of the tangential velocity α_i^j by discretization of (7). Then the values of η_i^j are computed and used for updating local lengths r_i^j by discretizing Eq. (11). Using computed local lengths, the intrinsic derivatives are approximated in (10), and (12), and pentadiagonal systems with periodic boundary conditions are constructed and solved for new discrete curvatures k_i^j and position vectors x_i^j.

In order to discretize (7) we integrate it over flowing finite volume $\left[x_{i-1}, x_i\right]$ to obtain

$$\int_{x_{i-1}}^{x_i} \partial_s\alpha \,\mathrm{d}s = \int_{x_{i-1}}^{x_i} k\beta - \langle k\beta\rangle_\Gamma + \omega\,(L/g - 1)\,\mathrm{d}s.$$

Hence

$$\alpha_i - \alpha_{i-1} = r_i(k_i\beta_i - \langle k\beta\rangle_\Gamma) + \omega\,(L/n - r_i)$$

where $\alpha_0 = 0$. Taking discrete time stepping in the previous relation we obtain following expression for discrete values of the tangential velocity:

$$\alpha_i^j = \alpha_{i-1}^j + r_i^{j-1}(k_i^{j-1}\beta_i^{j-1} - B^{j-1}) + \omega\left(\frac{L^{j-1}}{n} - r_i^{j-1}\right)$$

where, for $i = 1,\ldots,n$,

$$\beta_i^j = -\frac{1}{r_i^j}\left(\frac{k_{i+1}^j - k_i^j}{q_i^j} - \frac{k_i^j - k_{i-1}^j}{q_{i-1}^j}\right) - \frac{1}{2}\left(k_i^j\right)^3,$$

$$q_i^j = \frac{1}{2}\left(r_i^j + r_{i+1}^j\right), \quad L^j = \sum_{l=1}^{n} r_l^j, \quad B^j = \frac{1}{L^j}\sum_{l=1}^{n} r_l^j k_l^j \beta_l^j,$$

and $\alpha_0^j = 0$, i.e. the point x_0^j is moved in the normal direction.

Now, a similar approximation methodology is applied for equation (11). Thus

$$r_i^{j-1}\frac{\eta_i^j - \eta_i^{j-1}}{\tau} = -r_i^{j-1}k_i^{j-1}\beta_i^{j-1} + \alpha_i^j - \alpha_{i-1}^j$$

for $i = 1,\ldots,n$. It leads to the update formula for local lengths:

$$r_i^j = \exp(\eta_i^j), \quad i = 1,\ldots,n,$$

subject to periodic boundary conditions $r_{-1}^j = r_{n-1}^j$, $r_0^j = r_n^j$, $r_{n+1}^j = r_1^j$, $r_{n+2}^j = r_2^j$. New local lengths are used for approximation of intrinsic derivatives in the curvature Eq. (10). We obtain $\int_{x_{i-1}}^{x_i}\partial_t k\,\mathrm{d}s = \int_{x_{i-1}}^{x_i} -\partial_s^4 k - \frac{1}{2}\partial_s^2(k^3) + \partial_s(\alpha k)\,\mathrm{d}s + \int_{x_{i-1}}^{x_i} k(k\beta - \partial_s\alpha)\,\mathrm{d}s$. Hence

$$r_i\frac{\mathrm{d}k_i}{\mathrm{d}t} = -\left[\partial_s^3 k\right]_{x_{i-1}}^{x_i} - \frac{1}{2}\left[\partial_s(k^3)\right]_{x_{i-1}}^{x_i} + [\alpha k]_{x_{i-1}}^{x_i} + k_i(r_i k_i\beta_i - (\alpha_i - \alpha_{i-1})) \tag{15}$$

and taking semi-implicit time stepping, i.e. replacing time derivative by backward difference and treating linear terms at the current time level j while the nonlinear terms at the level $j-1$, and approximating derivative terms on the boundaries of flowing finite volumes by finite differences we obtain

following pentadiagonal system with periodic boundary conditions for new discrete values of the curvature:

$$a_i^j k_{i-2}^j + b_i^j k_{i-1}^j + c_i^j k_i^j + d_i^j k_{i+1}^j + e_i^j k_{i+2}^j = f_i^j \tag{16}$$

for $i = 1, \ldots, n$, subject to periodic boundary conditions $k_{-1}^j = k_{n-1}^j, k_0^j = k_n^j, k_{n+1}^j = k_1^j, k_{n+2}^j = k_2^j$. For completeness, a detailed description of the system coefficients is given in Appendix.

Finally we discretize Eq. (12) by integrating in a dual volume $\left[\tilde{x}_{i-1}, \tilde{x}_i\right]$ to get

$$\int_{\tilde{x}_i}^{\tilde{x}_{i+1}} \partial_t x \, \mathrm{d}s = \int_{\tilde{x}_i}^{\tilde{x}_{i+1}} -\partial_s^4 x - \frac{3}{2}\partial_s(k^2 \partial_s x) + \alpha \partial_s x \, \mathrm{d}s,$$

$$q_i \frac{\mathrm{d}x_i}{\mathrm{d}t} = \left[-\partial_s^3 x - \frac{3}{2}k^2 \partial_s x\right]_{\tilde{x}_i}^{\tilde{x}_{i+1}} + \alpha_i(\tilde{x}_{i+1} - \tilde{x}_i).$$

Now replacing the time derivative by the backward difference, derivative terms on boundaries of dual volume by finite differences and $\tilde{x}_i$ by the average of grid points in the last term, we obtain two tridiagonal systems for updating the position vector:

$$\mathcal{A}_i^j x_{i-2}^j + \mathcal{B}_i^j x_{i-1}^j + \mathcal{C}_i^j x_i^j + \mathcal{D}_i^j x_{i+1}^j + \mathcal{E}_i^j x_{i+2}^j = \mathcal{F}_i^j \tag{17}$$

$i = 1, \ldots, n$, subject to periodic boundary conditions $x_{-1}^j = x_{n-1}^j, x_0^j = x_n^j, x_{n+1}^j = x_1^j, x_{n+2}^j = x_2^j$. The exact form of coefficients $\mathcal{A}, \mathcal{B}, \mathcal{C}, \mathcal{D}, \mathcal{E}$ can be found in Appendix.

The initial quantities for the algorithm are computed from discrete representation of the initial curve x_0. The reader is referred to [19] for further details. Every pentadiagonal system is solved by Gauss-Seidel iterates. We stop the Gauss-Seidel iteration procedure if a difference of subsequent iterates in maximum norm is less than the prescribed tolerance 10^{-10}.

3.2 Numerical approximation of the level set method

Concerning approximation of the level set Eq. (13) we consider rectangular domain $\Omega \equiv \langle a_1, a_2\rangle \times \langle b_1, b_2\rangle$ and we assume an equidistant spatial step h in both directions. We define a regular mesh ω_h consisting of grid points $x_{ij} = [a_1 + ih, b_1 + jh]$ for $i = 0, \ldots, N_1$, $j = 0, \ldots, N_2$, where $a_1 + N_1 h = a_2$ and $b_1 + N_2 h = b_2$. Without loss of generality we shall assume $a_1 = b_1 = 0$. The corresponding dual mesh $\mathcal{V}$ is given as the union of the finite volumes V_{ij} of the form $\left\langle \left(i - \frac{1}{2}\right)h, \left(i + \frac{1}{2}\right)h\right\rangle \times \left\langle \left(j - \frac{1}{2}\right)h, \left(j + \frac{1}{2}\right)h\right\rangle$ for $i = 0, \ldots, N_1$, $j = 0, \ldots, N_2$. The projection of a solution at x_{ij} is defined as $u_{ij} = u(x_{ij})$. Similarly as in the Lagrangian method we take a uniform division of the time interval $[0, T]$ with a time step $\tau = \frac{T}{m}$. Let us consider an element V_{ij} of the dual mesh $\mathcal{V}$. Integrating (13)-(14) over V_{ij} and applying the Stokes theorem we obtain

$$\int_{V_{ij}} \frac{1}{Q}\frac{\partial u}{\partial t}\mathrm{d}x = \int_{\partial V_{ij}} \frac{1}{2}\frac{w^2}{Q^3}\frac{\partial u}{\partial \nu} - \langle \mathbb{E}\nabla w, \nu\rangle \, \mathrm{d}\sigma, \tag{18}$$

$$\int_{V_{ij}} \frac{w}{Q}\mathrm{d}x = \int_{\partial V_{ij}} \frac{1}{Q}\frac{\partial u}{\partial \nu}\mathrm{d}\sigma \tag{19}$$

where ν is the outer normal of the boundary ∂V_{ij}.

We start with approximation of the term Q on V_{ij}. For $r, s \in \{-1, 1\}$, $|r| + |s| = 1$, we define the linear operator ∇^{rs} as follows:

$$\nabla^{r,0} u_{ij} = \frac{1}{h}\left(r(u_{i+r,j} - u_{ij}), u_{ij}^{r,1} - u_{ij}^{r,-1}\right),$$

$$\nabla^{0,s} u_{ij} = \frac{1}{h}\left(u_{ij}^{1,s} - u_{ij}^{-1,s}, s(u_{i,j+s} - u_{ij})\right)$$

where u_{ij}^{rs} is the average of u_{ij} defined as:

$$u_{ij}^{rs} = \frac{1}{4}(u_{ij} + u_{i+r,j} + u_{i,j+s} + u_{i+r,j+s}).$$

For a fixed regularization parameter $0 < \epsilon \ll 1$ we define

$$Q_{ij}^{rs;n} = \sqrt{\epsilon^2 + |\nabla^{rs} u_{ij}^n|^2}, \quad \bar{Q}_{ij}^n = \frac{1}{4}\sum_{|r|+|s|=1} Q_{ij}^{rs;n}.$$

Let $\mathbb{E}_{ij}^{rs;n} = \left(E_{kl;ij}^{rs;n}\right)_{k,l=1,2}$ be the 2×2 projection matrix:

$$\mathbb{E}_{ij}^{rs;n} = \frac{1}{Q_{ij}^{rs;n}}\left(\mathbb{I} - \frac{\nabla^{rs} u_{ij}^n}{Q_{ij}^{rs;n}} \otimes \frac{\nabla^{rs} u_{ij}^n}{Q_{ij}^{rs;n}}\right).$$

Now we are able to derive a discretization of (18)

$$\frac{u_{ij}^n - u_{ij}^{n-1}}{\tau} = \frac{\bar{Q}_{ij}^{n-1}}{2h^2}\sum_{|r|+|s|=1} \frac{(\hat{w}_{ij}^{rs;n-1})^2}{(Q_{ij}^{rs;n-1})^3}(u_{i+r,j+s}^n - u_{ij}^n) - \frac{\bar{Q}_{ij}^{n-1}}{h^2}\sum_{|r|+|s|=1} h\langle \mathbb{E}_{ij}^{rs,n-1}\nabla^{rs} w_{ij}^n, \nu_{rs}\rangle \tag{20}$$

where

$$\hat{w}_{ij}^{rs;n} = \frac{1}{2}\left(w_{ij}^n + w_{i+r,j+s}^n\right), \tag{21}$$

and ν_{rs} is the unit outer normal vector, $\nu_{rs} = (r, s)$ for $|r| + |s| = 1$. In order to approximate w^n and w^{n-1} on V_{ij} and on its boundary ∂V_{ij} we have used expression (19) to obtain

$$w_{ij}^n = \frac{\bar{Q}_{ij}^n}{h^2}\sum_{|r|+|s|=1} \frac{1}{Q_{ij}^{rs;n}}(u_{i+r,j+s}^n - u_{ij}^n). \tag{22}$$

Since (20) contains a new time level w^n expressed through new time level of the solution u^n (see (22)) as well as the previous time level w^{n-1}, the resulting discrete level set scheme is semi-implicit in time. After some calculations it can be written as twenty one points scheme of the form

$$\sum_{(r,s)\in\mathcal{O}} A_{ij}^{rs} u_{i+r,j+s}^{n} = u_{ij}^{n-1} \tag{23}$$

where $\mathcal{O} = \{(r,s), -2 \le r,s \le 2, |r|+|s| < 4\}$ and $i = 2,\ldots,N_1-2$, $j = 2,\ldots,N_2-2$. For the remaining i, j, the values of u_{ij}^n are linearly extrapolated. The coefficients of the above system can be found in Appendix.

System (23) is solved by the iterative GMRES algorithm with ILUT (ILU with threshold) preconditioning or by the complete LU decomposition as a direct solver (cf. [23]). The time step τ is chosen to be proportional to h^2 and the regularization parameter ϵ can chosen either as a function of h or ϵ can be prescribed as a small fixed constant. As an initial condition we choose a signed distance function $d(x)$ to the initial curve. At prescribed redistancing time steps we perform redistancing of the level set solution back to the signed distance using the fast sweeping method (see [24] for details). As an alternative to the semi-implicit scheme (20) we may also consider its explicit version, i.e. all the terms on the right hand side of (20) are considered at the time step $n-1$, c.f. [1,21] for other similar explicit schemes. In this case we avoid the singularities of the signed distance function in its local extrema and the initial condition has a "phase-field" like shape

$$u^0(x) = \delta \mathrm{sgn}(d(x))(1-\exp(-|d(x)/\delta|),$$

where δ is a parameter describing the width of the region where u^0 changes from $-\delta$ to $+\delta$.

4 Discussion on numerical experiments

4.1 Experimental order of convergence for the methods

Let an initial curve be a circle with radius r_0. Since for the circle we have $k = \frac{1}{r}$ then it follows from (2) that $\dot{r}(t) = \frac{1}{2} r(t)^{-3}$. Hence $r(t) = (2t + r_0^4)^{\frac{1}{4}}$. Using this simple analytical solution we can compute experimental order of convergence for both schemes. Without loss of generality we choose $r_0 = 1$.

In the case of the Lagrangian scheme we approximate the initial unit circle subsequently by $n = 10, 20, 40$ and 80 nodes with $h = 1/n$. The final time was set up to be $T = 2.56$ and time step was chosen to be proportional to h^2, i.e. $\tau = h^2$. Table 1 shows errors and experimental order of convergence (EOC) of the scheme in $L^p = L^p((0,T), L_p(S^1)) = L^p(S^1 \times (0,T))$ for $p = 2, \infty$.

Table 1 EOC for the Lagrangian scheme in L^p, $p = 2, \infty$ norms

Error / EOC \ h	0.1	0.05	0.025	0.0125
$p = 2$	0.04301	0.01089	0.00271	0.00067
EOC		1.982	2.005	2.003
$p = \infty$	0.03402	0.00886	0.00223	0.00056
EOC		1.940	1.986	1.988

Table 2 EOC for the level set scheme in L^p, $p = 2, \infty$ norms

Error / EOC \ h	0.4	0.2	0.1	0.05
$p = 2$	0.21497	0.06585	0.01699	0.00400
EOC		1.707	1.954	2.086
$p = \infty$	0.71190	0.12286	0.03780	0.00973
EOC		2.534	1.700	1.957

In the level set approximation we solve the problem in domain $\Omega = \langle -2,2\rangle \times \langle -2,2\rangle$. The domain Ω was splitted subsequently into $n \times n$ finite volumes for $n = 10, 20, 40, 80$ with $h = 1/n$. The final time was chosen as $T = 0.5$ and again $\tau = h^2$. The regularization parameter ϵ was refined proportionally to the grid refinement using the rule $\epsilon^2 = 2h$. Finally, the redistancing period was $\tau_{redist} = 0.25h$. Errors in L^p, $p = 2, \infty$ norms are presented in Table 2.

4.2 Comparison of the Lagrangian and the level set evolutions

In this section we compare the numerical results obtained by our Lagrangian and the level set approaches on various representative examples. In the case of Lagrangian scheme we approximate an evolving curve by 100 grid nodes in all experiments to follow. In the case of the level set method we hereafter split domain Ω into 100×100 finite volumes.

In Fig. 1 we present comparison of both methods for the case of evolution of an initial circle with the radius $r_0 = 1$. The time horizon $T = 0.5$. By cross marks we depict approximation by the Lagrangian direct scheme where the evolution was computed using the time step $\tau = 0.002$ and no tangential redistribution ($\alpha = 0$). The evolution of the level set function was computed in the spatial domain $\Omega = \langle -2,2\rangle \times \langle -2,2\rangle$ with the time step $\tau = 0.002$ and the smoothing parameter $\epsilon = 0.001$. We did not provide redistancing in this case in order to show deformation of an initial distance function to final shape of the level set function (see Fig. 1 bottom).

In Fig. 2 we show evolution of an initial ellipse with half-axes 1 and 2. It asymptotically approaches a circle. We stop computations at the time horizon $T = 2.56$. In the case of the Lagrangian approach we pick $\tau = 0.002$ and the

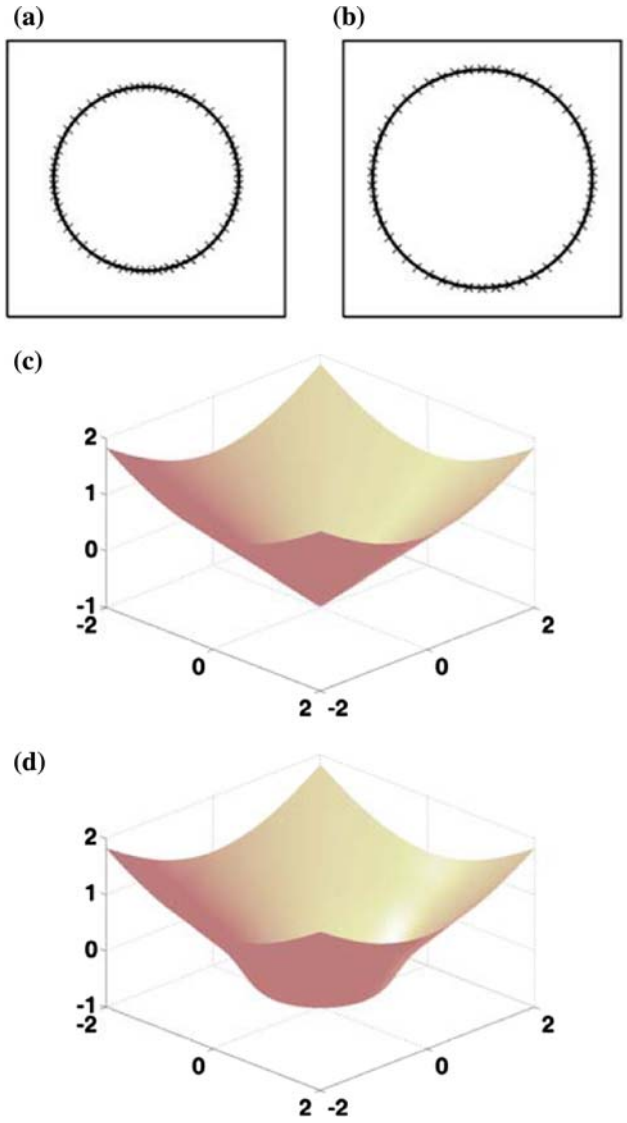

Fig. 1 **a** A *circle* as an initial condition; **c** the same initial condition for the level set approximation; **b** a *circle* computed at the time $T = 0.5$ by both methods (*cross marks* correspond to the Lagrangian method); **d** the level set function at the time $T = 0.5$

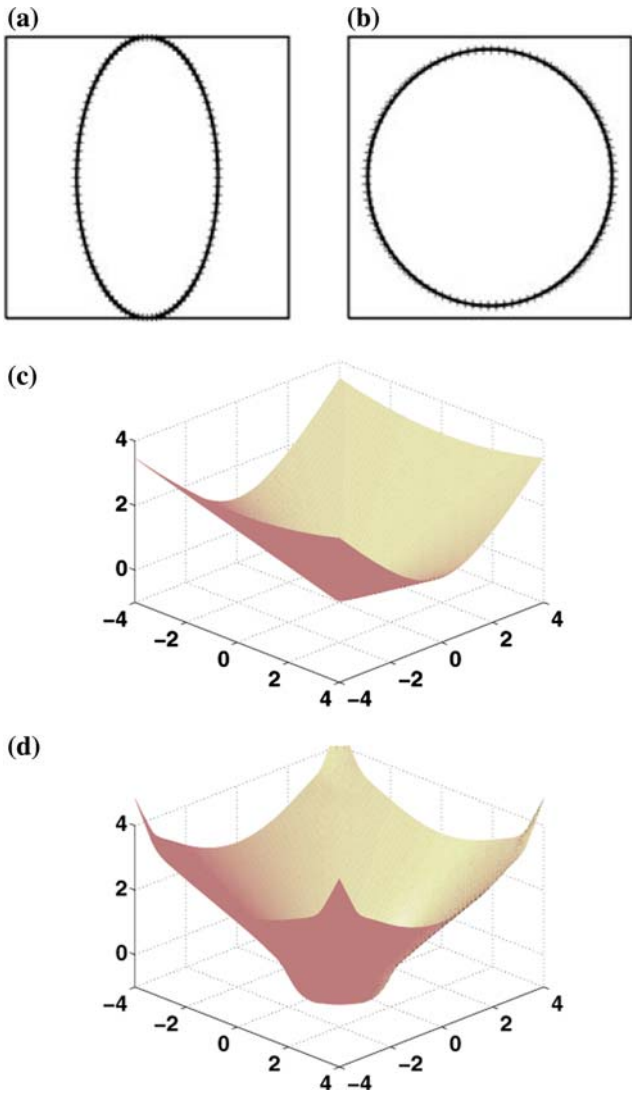

Fig. 2 **a** An initial *ellipse with half-axes* ratio 1:2; **c** the same initial condition for the level set approximation; **b** the approximate *circle* computed at the time $T = 2.56$ by both methods (*cross marks* correspond to the Lagrangian method); **d** the level set function at the time $T = 2.56$

tangential redistribution parameter $\omega = 1$. We computed evolution of the level set function in the computational domain $\Omega \equiv \langle -4, 4\rangle \times \langle -4, 4\rangle$. We chose the smoothing parameter $\epsilon = 0.001$ and we did redistancing just once at $\tau_{redist} = T/2$. Both, the initial and final level set functions are depicted in Fig.2.

In Fig. 3 (top) the initial condition is a non-convex curve given by

$$x^0(u) = \begin{pmatrix} 1 - 0.5\cos^2(4\pi u)\cos(2\pi u) \\ 1 - 0.5\cos^2(4\pi u)\sin(2\pi u) \end{pmatrix} \tag{24}$$

where $0 \le u \le 1$. The time evolution of such a non-convex initial curve was stopped at the time $T = 0.01$. In the Lagrangian approach we picked $\tau = 10^{-5}$, and the tangential redistribution parameter was $\omega = 1$. The level set function was computed in the domain $\Omega \equiv \langle -2, 2\rangle \times \langle -2, 2\rangle$, with $\tau = 2.5 \cdot 10^{-5}$, $\epsilon = 0.001$ and $\tau_{redist} = 0.001$. Again, a comparison of the zero level set and the initial curve evolved by Lagrangian method show compatibility of both methods in the common time interval. In this example the Willmore flow quickly changes the shape of evolving curves from non-convex to a circular one. We show several time steps of the curve evolution in Fig. 3.

In Fig. 4 we present evolution with the initial curve having sharp corners (see also a detailed close-up in Fig. 5). Although the initial curve (square) is convex, the evolved curve need not be convex for small times. Concerning

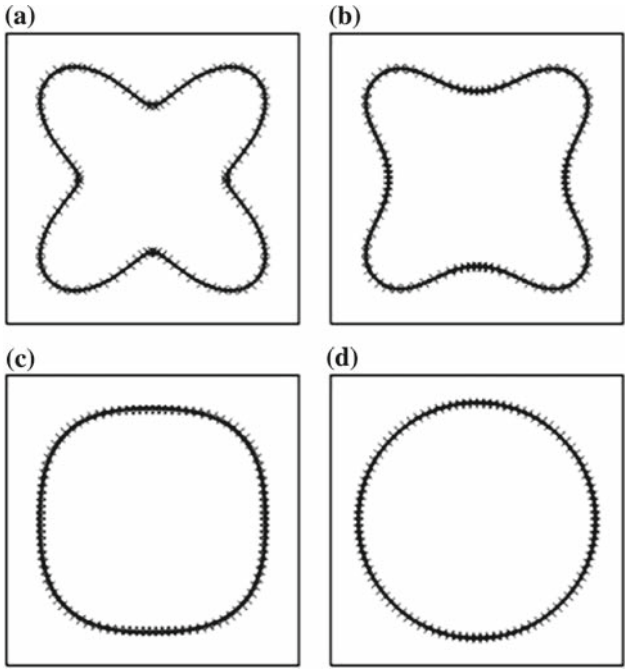

Fig. 3 An initial condition **a** given by (24) and *curves* computed by both methods at **b**: $t = 0.001$, **c**: $t = 0.005$ and **d**: $t = 0.01$

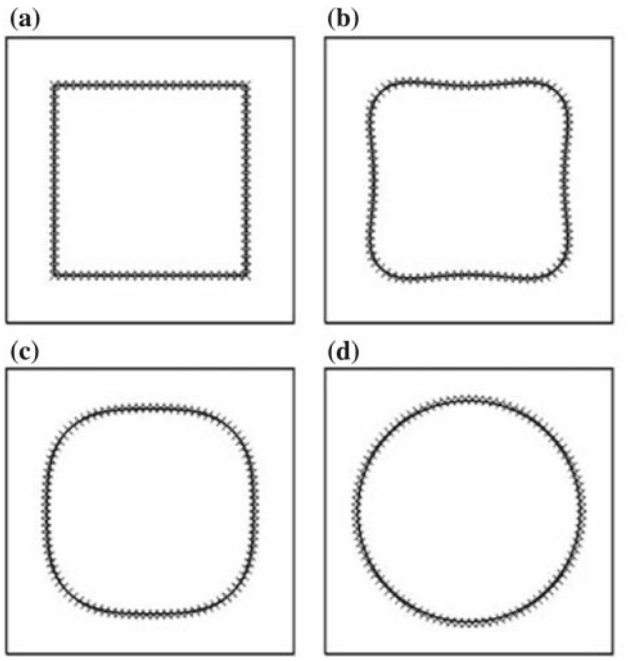

Fig. 4 A *square* as an initial condition **a** and *computed evolved curves* **b**: $t = 0.001$, **c**: $t = 0.01$ and **d**: $t = 0.1$

numerical parameters, we chose $n = 100$ spatial nodes, $\tau = 10^{-7}$ and the tangential redistribution parameter $\omega = 1$ (asymptotically uniform redistribution) in the direct Lagrangian method. As for the level-set method we took $h = 0.04$, $\tau = 2.5 \cdot 10^{-5}$, $\epsilon = 10^{-5}$ and $\tau_{redist} = 0.01$.

Figure 6 shows comparison of the methods for another non-convex curve with very sharp corners. We chose the same

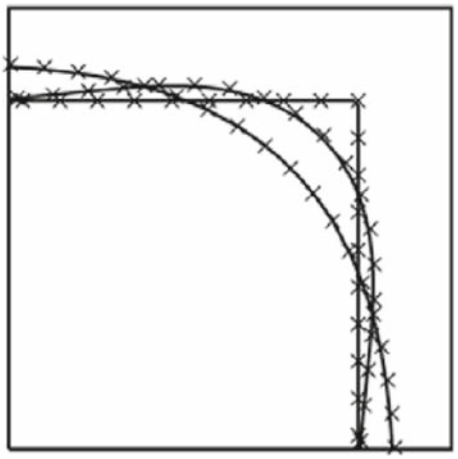

Fig. 5 The detail of the *square corner* at the times $t = 0, 0.001$ and $t = 0.01$

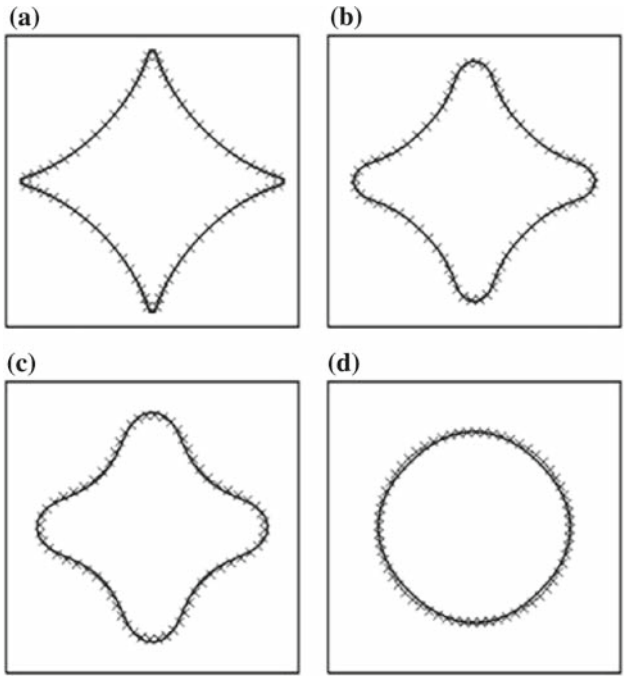

Fig. 6 An *asteroid* as an initial condition **a** and its evolution at **b**: $t = 0.0001$; **c**: $t = 0.0005$ and **d**: $t = 0.005$

numerical parameters as in the previous example for both the Lagrangian as well as level set methods. Also in this example one can observe satisfactory coincidence of numerically computed curves by both methods.

Finally, in Fig. 7 we present an example illustrating a topological change. It has been computed by the level set method only because the direct method is unable to handle topological changes like pinching and splitting of curves. The initial zero level set consists of two almost touching curves - the inner curve being a circle and the outer curve being an ellipse with a shorter axis just slightly larger than the radius of the inner circle. We then let evolve this configuration by the level

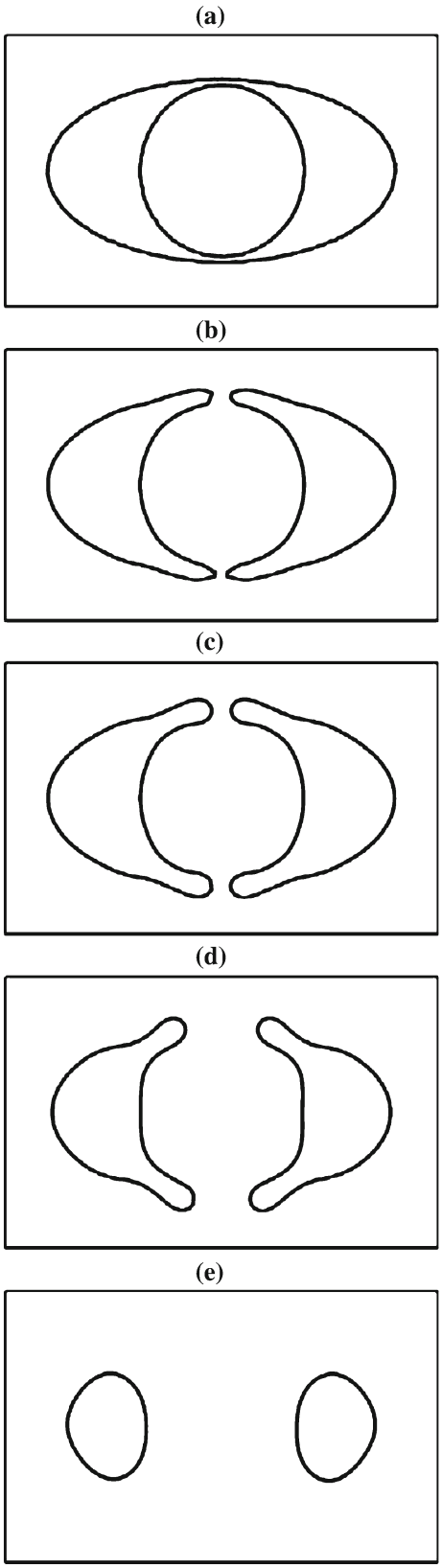

Fig. 7 From *top to bottom* initial condition composed of two curves—a *circle* within an *ellipse* **a** and its evolution at **b**: $t = 0.00006$; **c**: $t = 0.0002$; **d**: $t = 0.002$ and **e**: $t = 0.008$

set equation. The phenomenon of pinching and subsequent splitting of the evolved curves can be observed in this example. Such a behavior can be observed in the mean curvature driven evolution of a dumb-bell initial surface in 3D where the Grayson theorem does not hold. To our best knowledge, there is no analytical proof of pinching-splitting phenomenon in the case of a Willmore flow of planar curves. Notice that this numerical result has been obtained only by using very small time steps, in the range $10^{-11} - 10^{-10}$. Since for such small time steps we do not increase efficiency by using the semi-implicit scheme we use here its explicit version with the Runge–Kutta–Merson fourth order adaptive time solver. As further parameters we used $h = 0.0166$, $\epsilon = 10^{-5}$ and $\tau_{redist} = 10^{-5}$.

Acknowledgments The authors are thankful to the referee for her/his valuable comments and suggestions that helped us to improve the final version of the paper.

Appendix

Coefficients of the Lagrangean systems

The coefficients for the curvature system (16) are as follows:

$$a_i^j = \frac{1}{q_{i-1}^j r_{i-1}^j q_{i-2}^j}, \quad e_i^j = \frac{1}{q_i^j r_{i+1}^j q_{i+1}^j},$$

$$b_i^j = -\left(\frac{1}{r_i^j q_i^j q_{i-1}^j} + \frac{1}{r_i^j (q_{i-1}^j)^2} + \frac{1}{(q_{i-1}^j)^2 r_{i-1}^j} + \frac{1}{q_{i-1}^j r_{i-1}^j q_{i-2}^j}\right) + \frac{\alpha_{i-1}^j}{2},$$

$$d_i^j = -\left(\frac{1}{q_i^j r_{i+1}^j q_{i+1}^j} + \frac{1}{(q_i^j)^2 r_{i+1}^j} + \frac{1}{r_i^j (q_i^j)^2} + \frac{1}{r_i^j q_i^j q_{i-1}^j}\right) - \frac{\alpha_i^j}{2},$$

$$c_i^j = \frac{1}{(q_i^j)^2 r_{i+1}^j} + \frac{1}{r_i^j (q_i^j)^2} + \frac{2}{r_i^j q_i^j q_{i-1}^j} + \frac{1}{r_i^j (q_{i-1}^j)^2} + \frac{1}{(q_{i-1}^j)^2 r_{i-1}^j} + \frac{r_i^j}{\tau} - r_i^{j-1} k_i^{j-1} \beta_i^{j-1} + \frac{\alpha_i^j}{2} - \frac{\alpha_{i-1}^j}{2},$$

$$f_i^j = \frac{r_i^j}{\tau} k_i^{j-1} + \frac{(k_i^{j-1})^3 - (k_{i-1}^{j-1})^3}{2q_{i-1}^j} - \frac{(k_{i+1}^{j-1})^3 - (k_i^{j-1})^3}{2q_i^j}$$

where we used following approximation of third order derivative terms on boundaries of flowing finite volume in (15):

$$\partial_s^3 k(x_i) - \partial_s^3 k(x_{i-1}) \approx \approx \frac{\partial_s^2 k(\tilde{x}_{i+1}) - \partial_s^2 k(\tilde{x}_i)}{q_i} - \frac{\partial_s^2 k(\tilde{x}_i) - \partial_s^2 k(\tilde{x}_{i-1})}{q_{i-1}}$$

$$
\begin{aligned}
&\approx \cdots \approx \frac{1}{q_i r_{i+1} q_{i+1}} k_{i+2} + \frac{1}{q_{i-1} r_{i-1} q_{i-2}} k_{i-2} \\
&-\left(\frac{1}{q_i r_{i+1} q_{i+1}} + \frac{1}{q_i^2 r_{i+1}} + \frac{1}{r_i q_i^2} + \frac{1}{r_i q_i q_{i-1}} \right) k_{i+1} \\
&+\left(\frac{1}{q_i^2 r_{i+1}} + \frac{1}{r_i q_i^2} + \frac{2}{r_i q_i q_{i-1}} + \frac{1}{r_i q_{i-1}^2} + \frac{1}{q_{i-1}^2 r_{i-1}} \right) k_i \\
&-\left(\frac{1}{r_i q_i q_{i-1}} + \frac{1}{r_i q_{i-1}^2} + \frac{1}{q_{i-1}^2 r_{i-1}} + \frac{1}{q_{i-1} r_{i-1} q_{i-2}} \right) k_{i-1}.
\end{aligned}
$$

Using a similar strategy for approximation of the third order derivatives of position vector on boundaries of flowing dual volume we can write coefficients of (17):

$$
\begin{aligned}
\mathcal{A}_i^j &= \frac{1}{r_i^j q_{i-1}^j r_{i-1}^j}, \quad \mathcal{C}_i^j = \frac{q_i^j}{\tau} - (\mathcal{A}_i^j + \mathcal{B}_i^j + \mathcal{D}_i^j + \mathcal{E}_i^j), \\
\mathcal{E}_i^j &= \frac{1}{r_{i+1}^j q_{i+1}^j r_{i+2}^j}, \quad \mathcal{F}_i^j = \frac{q_i^j}{\tau} x_i^{j-1}, \\
\mathcal{B}_i^j &= -\left(\frac{1}{r_i^j q_{i-1}^j r_{i-1}^j} + \frac{1}{(r_i^j)^2 q_{i-1}^j} + \frac{1}{(r_i^j)^2 q_i^j} \right. \\
&\quad \left. + \frac{1}{r_i^j q_i^j r_{i+1}^j} \right) + \frac{3}{2} \frac{(k_i^j)^2}{r_i^j} + \frac{\alpha_i^j}{2}, \\
\mathcal{D}_i^j &= -\left(\frac{1}{r_i^j q_i^j r_{i+1}^j} + \frac{1}{(r_{i+1}^j)^2 q_i^j} + \frac{1}{(r_{i+1}^j)^2 q_{i+1}^j} \right. \\
&\quad \left. + \frac{1}{r_{i+1}^j q_{i+1}^j r_{i+2}^j} \right) + \frac{3}{2} \frac{(k_{i+1}^j)^2}{r_{i+1}^j} - \frac{\alpha_i^j}{2}.
\end{aligned}
$$

Coefficients of the level set system

The coefficients A_{ij}^{rs} of the 21-diagonal system matrix (23) are given by:

$$
\begin{aligned}
A_{ij}^{00} = 1 + \frac{\tau Q_{ij}}{h^4} \sum_{r,s \in \{-1,1\}} \Bigg[& \frac{h^2 \left(\hat{w}_{ij}^{rs;n-1} \right)^2}{2 \left(Q_{ij}^{rs;n-1} \right)^3} \\
& + E_{1+|s|,2-|r|;ij}^{r,s} \left(\frac{\bar{Q}_{i+r,j+s}^{n-1}}{Q_{i+r,j+s}^{-r,-s;n-1}} + \frac{\bar{Q}_{ij}^{n-1}}{Q_{ij}^{*;n-1}} \right) \\
& + \frac{1}{4} E_{1+|s|,1+|r|;ij}^{r,s} \left(\frac{\bar{Q}_{i+s,j+r}^{n-1}}{Q_{i+s,j+r}^{-r,-s;n-1}} - \frac{\bar{Q}_{i-s,j-r}^{n-1}}{Q_{i-s,j-r}^{sr;n-1}} \right) \Bigg],
\end{aligned}
$$

$$
\begin{aligned}
A_{ij}^{rs} = \frac{\tau}{h^4} \bar{Q}_{ij}^{n-1} \Bigg[& - E_{1+|s|,2-|r|;ij}^{rs;n-1} \left(\frac{\bar{Q}_{i+r,j+s}^{n-1}}{Q_{i+r,j+s}^{*;n-1}} + \frac{\bar{Q}_{ij}^{n-1}}{Q_{ij}^{rs;n-1}} \right) \\
& + \frac{1}{4} E_{1+|s|,1+|r|;ij}^{rs;n-1} \left(\frac{\bar{Q}_{i+r+s,j+r+s}^{n-1}}{Q_{i+r+s,j+r+s}^{-s,-r;n-1}} - \frac{\bar{Q}_{i+r-s,i-r+s}^{n-1}}{Q_{i+r-s,j-r+s}^{sr;n-1}} \right) \\
& + \frac{1}{4} E_{1+|r|,1+|s|;ij}^{sr;n-1} \left(\frac{\bar{Q}_{i+r+s,j+r+s}^{n-1}}{Q_{i+r+s,j+r+s}^{-s,-r;n-1}} - \frac{\bar{Q}_{i+r,j+s}^{n-1}}{Q_{i+r,j+s}^{*;n-1}} \right) \\
& - \frac{1}{4} E_{1+|r|,1+|s|;ij}^{-s,-r;n-1} \left(\frac{\bar{Q}_{i+r-s,j-r+s}^{n-1}}{Q_{i+r-s,j-r+s}^{sr;n-1}} - \frac{\bar{Q}_{i+r,j+s}^{n-1}}{Q_{i+r,j+s}^{*;n-1}} \right) \\
& - \left(E_{1+|s|,2-|r|;ij}^{-r,-s;n-1} + E_{1+|r|,2-|s|;ij}^{sr;n-1} \right. \\
& \left. + E_{1+|r|,2-|s|}^{-s,-r;n-1} \right) \frac{\bar{Q}_{ij}^{n-1}}{Q_{ij}^{rs;n-1}} - \frac{h^2 \left(\hat{w}_{ij}^{rs;n-1} \right)^2}{2 (Q_{ij}^{rs;n-1})^3} \Bigg],
\end{aligned}
$$

for $|r|+|s| = 1$. Here we have denoted by $Q_{i,j}^{*;n}$ the harmonic average of $Q_{ij}^{rs;n}$ defined as:

$$
\frac{1}{Q_{i,j}^{*;n}} = \sum_{|r|+|s|=1} \frac{1}{Q_{ij}^{rs;n}}.
$$

For $|r| = 1$ and $|s| = 1$ we have the expression:

$$
\begin{aligned}
A_{ij}^{rs} = rs \frac{\tau}{h^4} \bar{Q}_{ij}^{n-1} \Bigg[& \frac{E_{11;ij}^{r0;n-1} \bar{Q}_{i+r,j}^{n-1}}{Q_{i+r,j}^{0s;n-1}} + \frac{E_{22;ij}^{0s;n-1} \bar{Q}_{i,j+s}^{n-1}}{Q_{i,j+s}^{r0;n-1}} \\
& + \frac{1}{4} E_{12;ij}^{r0;n-1} \left(\frac{\bar{Q}_{i,j+s}^{n-1}}{Q_{i,j+s}^{r0;n-1}} - \frac{\bar{Q}_{i+r,j+s}^{n-1}}{Q_{i+r,j+s}^{*;n-1}} \right) \\
& + \frac{1}{4} E_{21;ij}^{0s;n-1} \left(\frac{\bar{Q}_{i+r,j}^{n-1}}{Q_{i+r,j}^{0s;n-1}} - \frac{Q_{i+r,j+s}}{Q_{i+r,j+s}^{*;n-1}} \right) \\
& - \frac{1}{4} \frac{E_{12;ij}^{-r,0;n-1} \bar{Q}_{i,j+s}^{n-1}}{Q_{i,j+s}^{r,0;n-1}} - \frac{1}{4} \frac{E_{21;ij}^{0,-s;n-1} \bar{Q}_{i+r,j}^{n-1}}{Q_{i+r,j}^{0,s;n-1}} \Bigg].
\end{aligned}
$$

Next, for $|r| = 2$ or $|s| = 2$ such that $|r| + |s| = 2$ we have

$$
\begin{aligned}
A_{ij}^{rs} = \frac{\tau}{h^4} \bar{Q}_{ij}^{n-1} \Bigg(& E_{1+|\bar{s}|,1+|\bar{s}|;ij}^{\bar{r},\bar{s};n-1} + \frac{1}{4} E_{21;ij}^{\bar{s},\bar{r};n-1} \\
& - \frac{1}{4} E_{21;ij}^{-\bar{s},-\bar{r};n-1} \Bigg) \frac{\bar{Q}_{i+\tilde{r},j+\tilde{s}}^{n-1}}{Q_{i+\tilde{r},j+\tilde{s}}^{\tilde{r},\tilde{s};n-1}},
\end{aligned}
$$

and, finally for $|r| + |s| = 3$, we have

$$
A_{ij}^{rs} = \operatorname{sgn}(rs) \frac{\tau}{4h^4} \frac{\bar{Q}_{ij}^{n-1} \bar{Q}_{i+\bar{r},j+\bar{s}}^{n-1}}{Q_{i+\bar{r},j+\bar{s}}^{\tilde{r},\tilde{s};n-1}} \left(E_{12,ij}^{\bar{r},0;n-1} + E_{21,ij}^{0,\bar{s};n-1} \right),
$$

where we have denoted $\bar{r} = \operatorname{sgn}(r), \bar{s} = \operatorname{sgn}(s)$ and $\tilde{r} = r - \bar{r}, \tilde{s} = s - \bar{s}$.

References

1. Beneš, M.: Numerical solution for surface diffusion on graphs. In: Beneš, M., Kimura, M., Nakaki, T. (eds.) Proceedings of Czech Japanese Seminar in Appl. Math. 2005, COE Lecture Notes, Vol. 3, pp. 9–25. Faculty of Math., Kyushu University Fukuoka (2006)
2. Bänsch, E., Morin, P., Nochetto, R.: Surface diffusion of graphs: variational formulation, error analysis, and simulation. SIAM J. Numer. Anal. **42**, 773–799 (2004)
3. Barrett, J.W., Garcke, H., Nürnberg, R.: A parametric finite element method for fourth order geometric evolution equations. J. Comput. Phys. **222**, 441–467 (2007)
4. Citti, G., Sarti, A.: A cortical based model of perceptual completion in the roto-translation space. J. Math. Imaging Vis. **24**(3), 307–326 (2006)
5. Cahn, J.W., Taylor, J.E.: Surface motion by surface diffusion. Acta Metallica Materiala **42**, 1045–1063 (1994)
6. Clarenz, U., Diewald, U., Dziuk, G., Rumpf, M., Rusu, R.: A finite element method for surface restoration with smooth boundary conditions. Comput. Aided Geometric Des. **21**, 427–445 (2004)
7. Deckelnick, K., Grunau, H.-Ch.: Boundary value problems for the one-dimensional Willmore equation–almost explicit solutions Preprint 2005
8. Deckelnick, K., Dziuk, G.: Error analysis of a finite element method for the Willmore flow of graphs. Interf. Free Bound. **8**(1), 21–46 (2006)
9. Droske, M., Rumpf, M.: A level set formulation for Willmore flow. Interf. Free Bound. **6**(3), 361–378 (2004)
10. Dziuk, G., Kuwert, E., Schatzle, R.: Evolution of elastic curves in $\mathbb{R}^n$: existence and computation. SIAM J. Math. Anal. **33**, 1228–1245 (2002)
11. Euler, L.: Methodus Inveniendi Lineas Curvas: Additamentum I, De Curvis Elasticis. Opera Omnia, Zürich: Orell Fassli, Ser. **1**(24), 231–297 (1952)
12. Frolkovič, P., Mikula, K.: Flux-based level set method: a finite volume method for evolving interfaces. Appl. Numer. Math. (to appear) doi:10.1016/j.apnum.2006.06.002
13. Frolkovič, P., Mikula, K.: High-resolution flux-based level set method. SIAM J. Sci. Comp. (to appear)
14. Hou, T.Y., Lowengrub, J., Shelley, M.: Removing the stiffness from interfacial flows and surface tension. J. Comput. Phys. **114**, 312–338 (1994)
15. Kass, M., Witkin, A., Terzopulos, D.: Snakes: active contour models. Int. J. Comput. Vis. **1**, 321–331 (1987)
16. Kimura, M.: Numerical analysis for moving boundary problems using the boundary tracking method. Jpn J. Ind. Appl. Math. **14**, 373–398 (1997)
17. Mikula, K., Ševčovič, D.: Evolution of plane curves driven by a nonlinear function of curvature and anisotropy. SIAM J. Appl. Math. **61**, 1473–1501 (2001)
18. Mikula, K., Ševčovič, D.: A direct method for solving an anisotropic mean curvature flow of planar curve with an external force. Math. Methods Appl. Sci. **27**(13), 1545–1565 (2004)
19. Mikula, K., Ševčovič, D.: Computational and qualitative aspects of evolution of curves driven by curvature and external force. Comput. Visual. Sci. **6**, 211–225 (2004)
20. Mikula, K., Ševčovič, D.: Tangentially stabilized Lagrangean algorithm for elastic curve evolution driven by intrinsic Laplacian of curvature ALGORITMY 2005. In: Conference on Scientific Computing, Vysoke Tatry-Podbanske, Slovakia, 13-18 March 2005, Proceedings of contributed papers and posters, pp. 32–41 (2005)
21. Oberhuber, T.: Numerical Solution for the Willmore Flow of Graphs, In: Beneš, M., Kimura, M., Nakaki, T. (eds.) Proceedings of Czech Japanese Seminar in Appl. Math. 2005, COE Lecture Notes, Vol. 3, pp. 126–138. Faculty of Math., Kyushu University Fukuoka (2006)
22. Sethian, J.A.: Level Set Methods and Fast Marching Methods: Evolving Interfaces in Computational Geometry, Fluid Mechanics, Computer Vision, and Material Science. Cambridge University Press, New York (1999)
23. Saad, Y.: Iterative Methods for Sparse Linear Systems, 2nd edn. SIAM (2003)
24. Zhao, H.: Fast sweeping method for Eikonal equations. Math. Comput. **74**, 603–627 (2005)
25. Zhu, W., Chan, T.: A variational model for capturing illusory contours using curvature. J. Math. Imaging Vis. **27**(1), 29–40 (2007)